Supplementary Figures

Figure 5. **Samples from the FRGC database.** The FRGC database contains male and female face images of adults from different races, with multiple photographs for each subject, different facial expressions, and different hairstyles. The faces are generally displayed in a fronto-parallel fashion, although some did moderately vary in posture. All faces were displayed against a uniform gray background, and illumination conditions were homogeneous and without cast shadows.

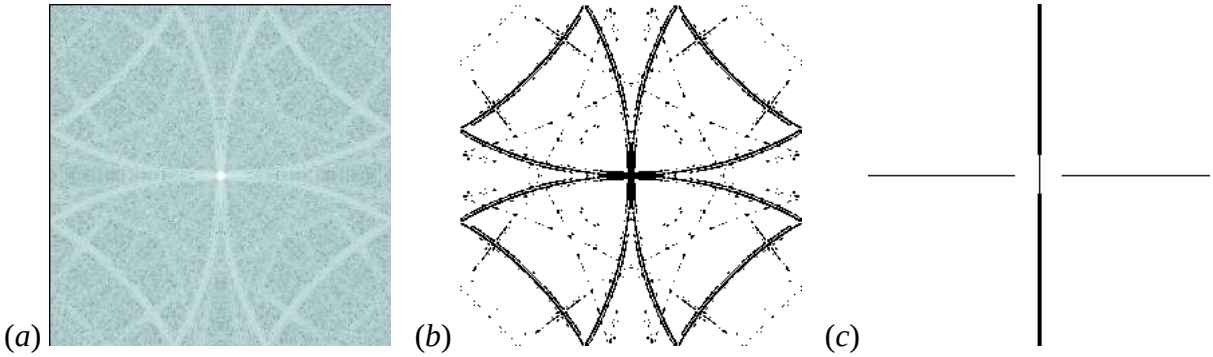

Figure 6. **Artifacts in the amplitude spectra.** (*a*) The log-amplitude-spectrum of the *minimum 4-term Blackman-Harris* (B.H.) window reveals a characteristic "fingerprint" (shown in this image), which also emerges when averaging a big number of amplitude spectra of B.H.-windowed faces. (*b*) The "fingerprint" is transformed into a binary image by thresholding with -0.25 (black color indicates values with 1, and white indicates 0). (*c*) Manually marked line artifacts which appear by averaging the amplitude spectra of a big number of face images (here without windowing).

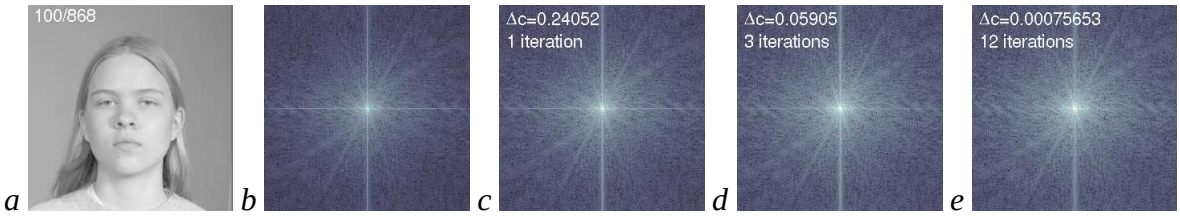

Figure 7. **Suppressing artifacts in the amplitude spectra.** This figure illustrates how artifacts in the amplitude spectra are suppressed by a nonlinear diffusion process, where the thresholded images of Supp. Fig. 6 served as spatially variant diffusion coefficient (see methods section). (*a*) Original face image. (*b*) The log-amplitude-spectrum of the image has horizontal and vertical lines which are generated as a consequence of truncating the shoulder region (c.f. Supp. Fig. 6*c*). (*c*) The spectrum after one iteration of nonlinear diffusion, with a difference in correlation to the original spectrum $\Delta c(1) \equiv c(0) - c(1) = 0.24052$. The spurious lines are already attenuated. (*d*) Three iterations with $\Delta c(3) = 0.05905$. (*e*) 12 iterations with $\Delta c(12) < 0.001$, which is the stopping criterion. The artificial lines are largely suppressed. The rest of the amplitude spectrum remains intact, and more interesting structures are now visible.

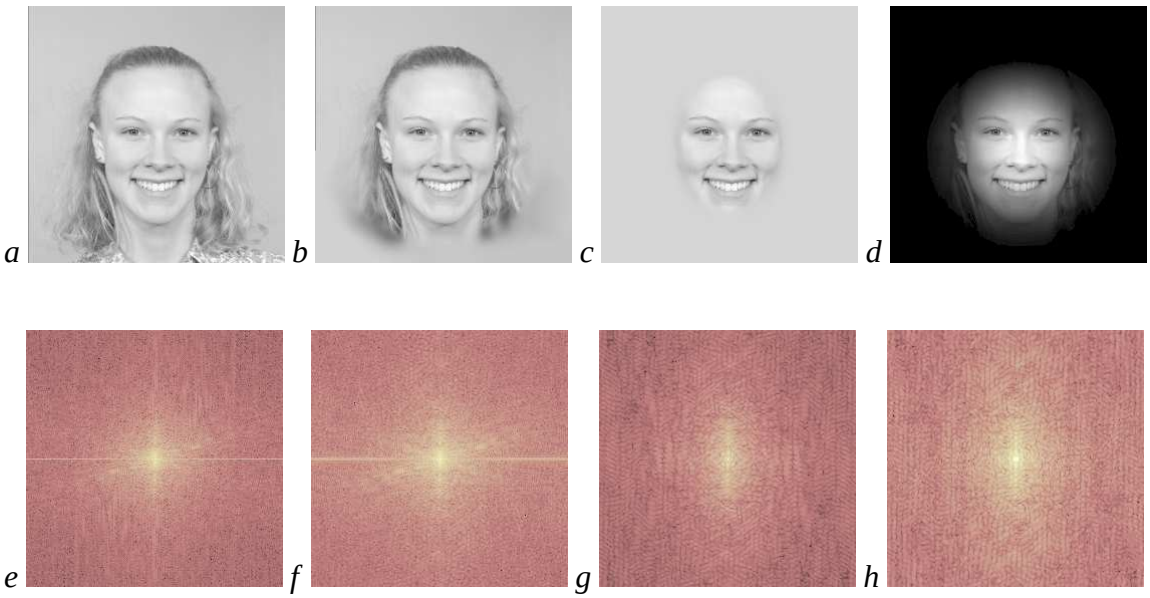

Figure 8. **Suppression of external face features.** The images in the bottom row (*e–h*) show the logarithmized amplitude spectra of the images (*a–d*) (face ID 104). The amplitude spectrum (*e*) of the original image (*a*) shows spurious horizontal and the vertical lines.(*b*) The spurious vertical line disappeared in the amplitude spectrum (*f*) when the shoulder region was manually erased, and the horizontal line then had a smaller amplitude. (*c*) Erasing all external face features led to the creation of a "moonface", thereby suppressing all of the artificial lines (*g*) . Finally, in (*d*) , a *minimum 4-term Blackman-Harris window* was centered at the nose position of the original image. The corresponding amplitude spectrum (*h*) of the windowed image is very similar to the amplitude spectrum of the "moonface" spectrum (but see Supp. Fig. 9).

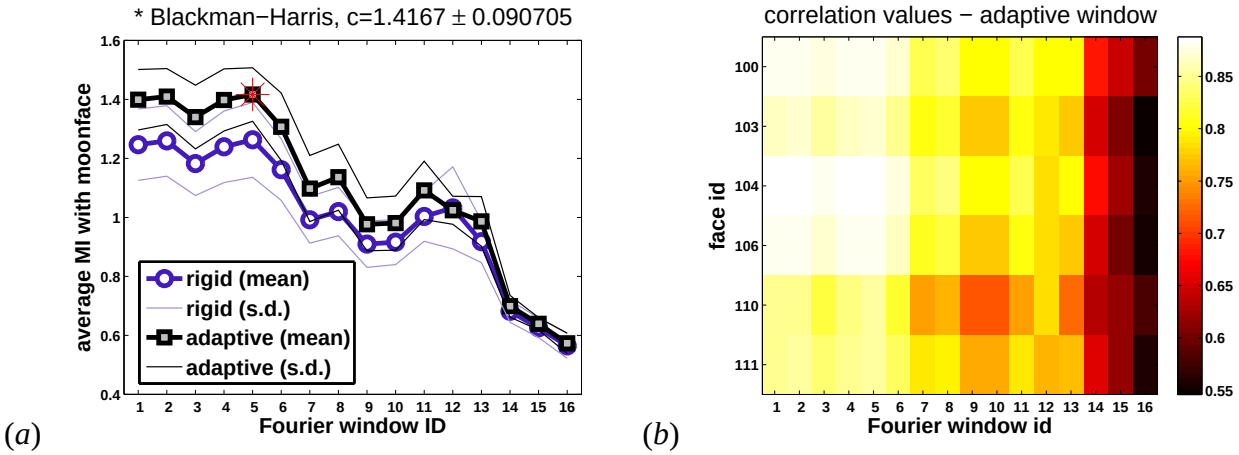

(*a*) (*b*)

Figure 9. **Similarities between the logarithmized amplitude spectra of "moonfaces" and windowed faces.** For six selected female images (with IDs indicated at the ordinate of panel *b*) which revealed strong line artifacts in their amplitude spectra, I computed similarity measures between the logarithmized amplitude spectra of corresponding "moonfaces" (e.g., Supp. Fig. 8*g*) and windowed faces (e.g., Supp. Fig. 8*h*; the window type is specified by the numbers at the abscissae).

(*a*) Mutual information averaged for the six images (mean ± s.d.). The center of the window was either positioned always at the center position of each image ("rigid"), or at the nose position with variable radius ("adaptive") – see legend. The *minimum 4-term Blackman-Harris window* scored the highest similarity (indicated by a red star). With correlation instead of mutual information, the curves show nearly the same relative similarities. In that case, the maximum average correlation value (± s.d.) was 0.87 ± 0.02 again for the adaptive *minimum 4-term Blackman-Harris window*.

(*b*) Individual correlation values for the adaptive window in a color code (color bar numbers indicate correlation values). The corresponding plot for mutual information is similar. The identification numbers ("Fourier-IDs") of the windows were 1=*Chebyshev window*, 2=*Nuttall-defined minimum 4-term Blackman-Harris window*, 3=*Bohman window*, 4=*Parzen (de la Valle-Poussin) window*, 5=*minimum 4-term Blackman-Harris window*, 6=*Blackman window*, 7=*modified Bartlett-Hann window*, 8=*Hann (Hanning) window*, 9=*triangular window*, 10=*Bartlett window*, 11=*Gaussian window*, 12=*flat top weighted window*, 13=*Hamming window*, 14=*Tukey (tapered cosine) window*, 15=*Kaiser window*, 16=*sharp-edged disk*.

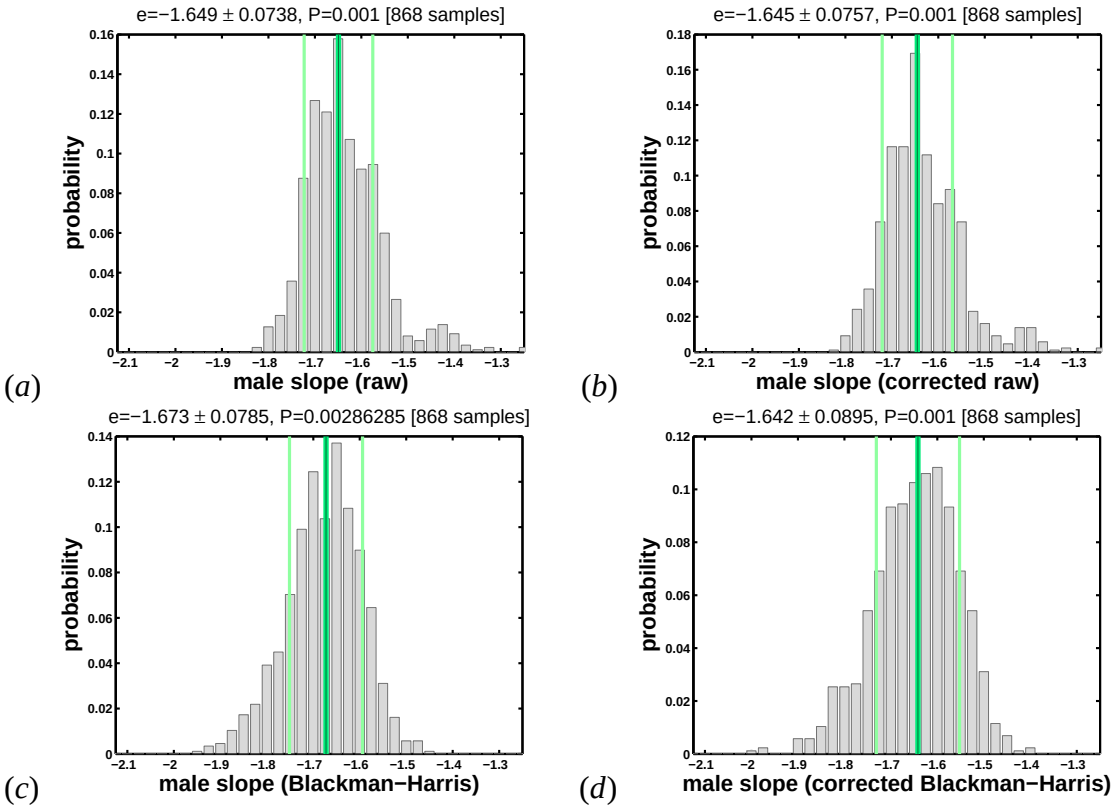

Figure 10. **Slopes for individual images (male faces).** The histograms show the probability of occurrence of slope values $e \equiv \alpha$ across all 868 male face images. For each face image, a corresponding slope value was obtained from fitting a line to the double-logarithmic representation of its isotropic 1-D amplitude spectrum (frequency range for fitting from 8 to 100 cycles per image, see Supp. Fig. 12). The centered vertical line in each histogram is the average α, and the flanking lines denote ± 1 s.d., respectively. A Jarque-Bera test was used to test the slope values for normal distribution (this test could be applied because of our large sample size) – corresponding P-values are indicated with each histogram. (*a*) Raw spectrum: $\alpha = -1.649 \pm 0.0738$, $P < 0.001$. (*b*) Corrected raw: $\alpha = -1.645 \pm 0.0757$, $P < 0.001$. (*c*) Blackman-Harris: $\alpha = -1.673 \pm 0.0785$, $P = 0.03$. (*d*) Corrected Blackman-Harris: $\alpha = -1.642 \pm 0.0895$, $P < 0.001$.

Supplementary figures

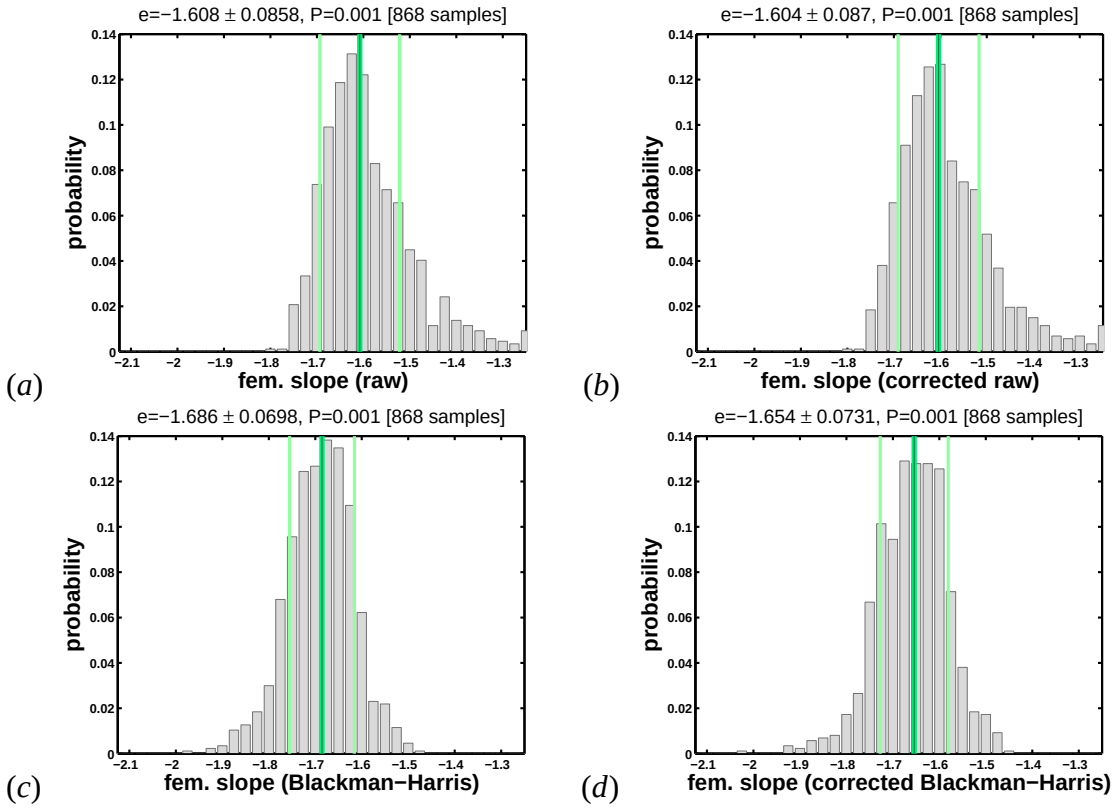

Figure 11. **Slopes for images of female faces.** Analogous to the previous figure, but here for the 868 female face images. (*a*) Raw spectrum: $\alpha = -1.608 \pm 0.0858$, $P < 0.001$. (*b*) Corrected raw: $\alpha = -1.604 \pm 0.0870$, $P < 0.001$. (*c*) Uncorrected Blackman-Harris window: $\alpha = -1.686 \pm 0.0.0698$, $P < 0.001$. (*d*) Corrected Blackman-Harris window: $\alpha = -1.654 \pm 0.0731$, $P < 0.001$.

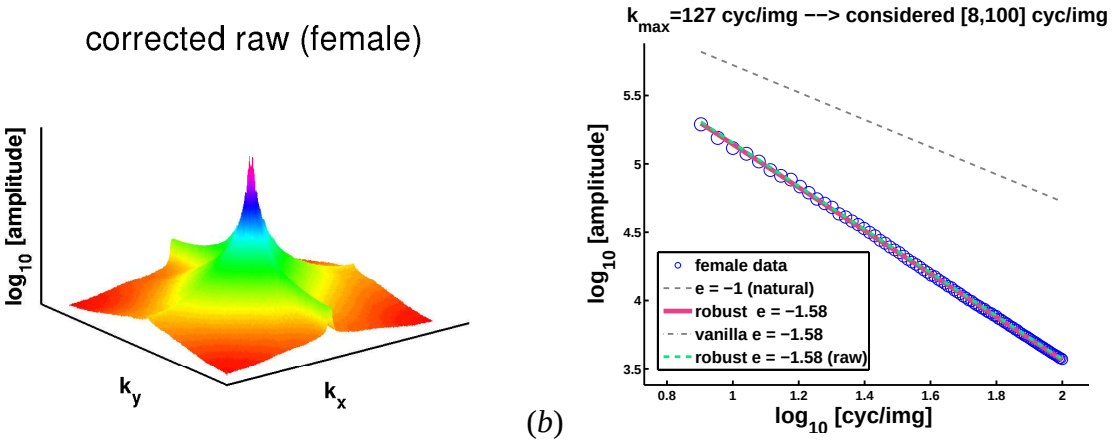

(*a*) (*b*)

Figure 12. **Mean amplitude spectrum I (corrected raw, female).** Same as Figure 1 in the main text, but here for the corrected raw amplitude spectrum of female faces. The size of circle symbols is proportional to their standard deviation (s.d.): maximum s.d. (biggest circle) was 28048.5 (18.1%), and the minium s.d. (smallest circle) was 987.916 (26.1%).

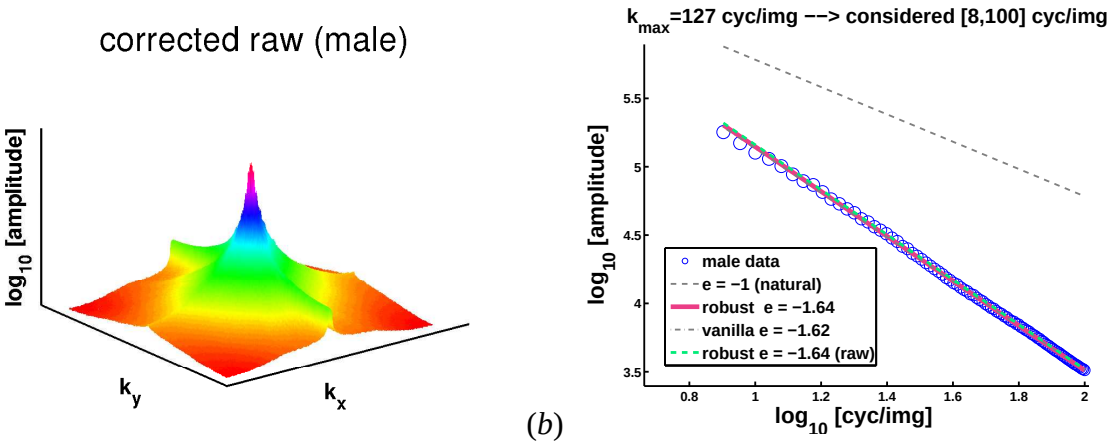

(*a*) (*b*)

Figure 13. **Mean amplitude spectrum II (corrected raw, male).** Same as Figure 1 in the main text, but here for the corrected raw amplitude spectrum of male faces. The size Maximum s.d. (biggest circle) was 26287.4 (14.7%), and the minium s.d. (smallest circle) was 991.628 (29.9%).

Supplementary figures

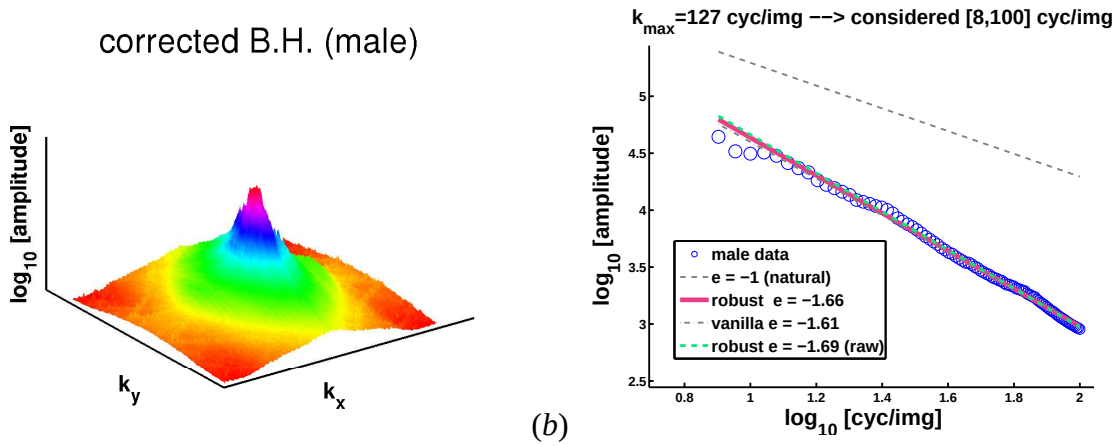

(*a*) (*b*)

Figure 14. **Mean amplitude spectrum III (corrected Blackman-Harris, male).** Analogous to Figure 1 but here for Blackman-Harris-windowed face images of males. As before, circles sizes are proportional to standard deviations, with a maximum standard deviation of 19519.3 (38.29%), and a minimum of 263.008 (28.9%).

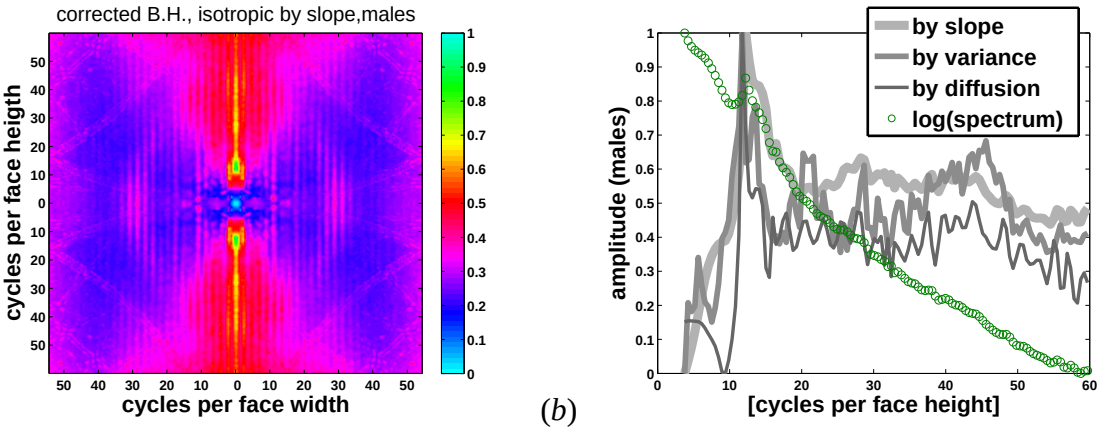

(*a*) (*b*)

Figure 15. **Whitening by slope.** Analogous to Figure 4, but for face images of males.

Supplementary figures

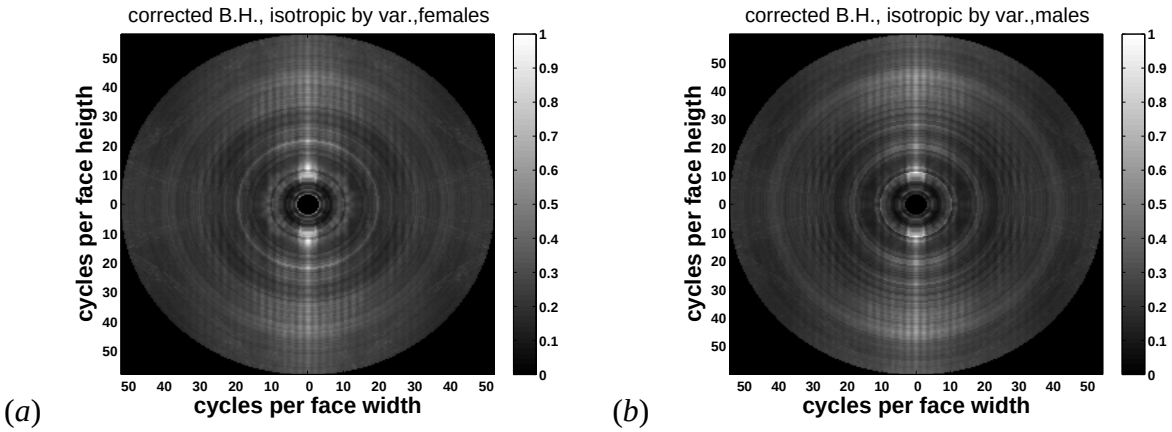

(*a*) (*b*)

Figure 16. **Whitening by variance.** Analogous to Figure 4(*a*) (females - left panel) and Figure 15(*a*) (males - right panel) but here for variance-whitening. Again, as with the slope-whitenend spectra, maxima are revealed at low spatial frequencies for horizontally oriented features (as indicated by the white regions close the center).